Science real and relevant conference 2010
Proceedings homepage://www.conference.csir.co.za/

Low-cost transparent solar cells: Potential of titanium dioxide nanotubes in the improvement of these next generation solar cells

Franscious Cummings[1,*], Lukas le Roux[1], Nomthandazo Mutangwa[1] and Dirk Knoesen[2]

[1]CSIR Materials Science and Manufacturing, Energy and Processes, PO Box 395, Pretoria, 0001
[2]Department of Physics, University of the Western Cape, Modderdam Road, Private Bag x17, Bellville, Cape Town 7535, South Africa

*Corresponding author: Franscious Cummings: fcummings@csir.co.za

Reference: EN15-PA-F

Abstract

In this work the synthesis of vertically aligned titanium dioxide (TiO_2) nanotubes was reported and investigated for their potential to increase the performance of dye-sensitised solar cells (DSCs). The nanotubes were synthesised by means of anodisation and it was found that the anodisation bath conditions had a direct influence on the morphology of the tubes. Tubes in excess of 10 µm and diameters greater than 50 nm were synthesised and their photovoltaic performance investigated.

1. Introduction

Dye-sensitised solar cells (DSCs) or Grätzel cells currently attract interest from scientific and industrial groups as they provide a low cost alternative to conventional silicon solar cells (O'Regan & Grätzel, 1991). In addition, DSCs show superior performance during cloudy days and use environmentally friendly materials (Toyoda et al., 2004). However, the light-to-electricity conversion efficiency of the best manufactured cells remains around the 10% mark, markedly lower than that of mono-crystalline silicon solar cells and currently poses as the biggest drawback in their large scale commercialisation. Recently it has been shown that the application of films of highly ordered, porous TiO_2 nanotubes has the potential to improve the overall efficiency of the cell. This is ascribed to the one-dimensional nature of nanotubes, which provide a linear transport route for electrons within the cell, which in turn, minimises the probability of scattering of these free charges as experienced by conventional DSCs (Paulose et al., 2006; Mor et al., 2006).

One distinct disadvantage of the TiO_2 nanotubes however, is their low surface area compared to a film of TiO_2 nanoparticles. As such much effort has been invested by our group to increase the surface area of the nanotubes. For application in DSCs, it has been found that of lengths in excess of 10 µm and diameters greater than 50 nm are required (Park et al., 2010). In order to achieve these tube dimensions, accurate control over the operating voltage and fluoride concentration need to be maintained during the anodisation process, which will be the focus of this investigation.

2. Experimental procedure

2.1 TiO_2 nanotube synthesis

The anodisation set-up employed during this study is based on a standard two-electrode set-up as previously reported (Cummings et al., 2010; Mohapatra et al., 2007). Ti foil samples (~ 1 x 1.5 cm^2, 25 µm thick, 99.99% purity, Advent Research Materials Ltd.) were cleaned with anhydrous ethanol, dried in a stream of nitrogen gas and cured at 80ºC for 10 minutes. Once dry, the Ti substrate (which serves as the

anode during anodisation) was immersed in an electrolyte solution comprising of ammonium fluoride (NH_4F) dissolved in deionised water (H_2O) and ethylene glycol (EG). A 1 x 1 cm^2 flag-shaped platinum (Pt) grid, which acted as the cathode during anodisation was then also immersed in the electrolyte solution, 1 cm away from the Ti foil. Hereafter the voltage was ramped to the desired value at a rate of 1 V/s. Based on previous experiments it was found that an optimum anodisation voltage of 60 V and a 2 wt% H_2O + 0.3 wt% NH_4F + EG electrolyte solution were required for the synthesis of TiO_2 nanotubes with length ~ 20 µm and diameter > 50 nm. All chemicals used during this study were of chemical grade and obtained from Merck (Pty) Ltd., South Africa.

2.2 Characterisation

The morphology of the nanotubes was studied with a high resolution JEOL JSM 7500F field emission scanning electron microscope (SEM) operated at electron beam energies between 1 and 10 keV. Atomic force microscopy (AFM) height images of the nanotubes were acquired using a Veeco NanoScope 124 IV Multi-Mode AFM in tapping mode. In order to investigate the crystallinity of the nanotubes, x-ray diffraction patterns were recorded with a PANalytical X'Pert Pro diffractometer, operated at 45 kV and 40 mA at the source. Copper, $K_{\alpha 1}$ radiation with a wavelength of 1.5406 Å was used as the x-ray source. A JEM-2100 JEOL high resolution transmission electron microscope (HR-TEM), operated at 100 kV was employed to examine the internal structure of the nanotubes samples. TEM samples were prepared by ultra-sonicating the annealed nanotube samples in isopropanol, where after a drop is placed on a holey-carbon copper grid and dried at ambient conditions. The current density-voltage (j-V) characteristics of the DSCs were measured under illumination using a Keithley 2420. The devices were irradiated at 100 mW cm^{-2} using a xenon lamp-based Sciencetech SF150 150 W solar simulator equipped with an AM1.5 filter as the white light source. The optical power at the sample was 100 mW cm^{-2}, as measured with a Daystar light meter. All the photovoltaic properties were evaluated in ambient air conditions at room temperature.

2.3 Manufacturing of lab-scale DSCs

Figure 1 shows the basic structure of the DSCs manufactured during this study. The cell consists of a working- and counter electrode. The working electrode consisted of a 20 x 15 mm^2 fluorine-doped tin oxide (FTO) coated glass substrate covered with a dense TiO_2 blocking layer and the dye-adsorbed TiO_2 nanoparticle (or nanotube) layer. The TiO_2 nanoparticle layer had dimensions of 9 x 5 mm^2. The counter electrode consisted of a 20 x 15 mm^2 glass-FTO substrate coated with a thin layer of Pt. The two electrodes were sealed by means of a hot-press, using a polymer adhesive, Surlyn® at 100ºC and a pressure of 1.5 bar. The electrolyte, which consists of an I^-/I_3^- redox couple, was then injected into the cell, where after the cell was sealed with the Surlyn®.

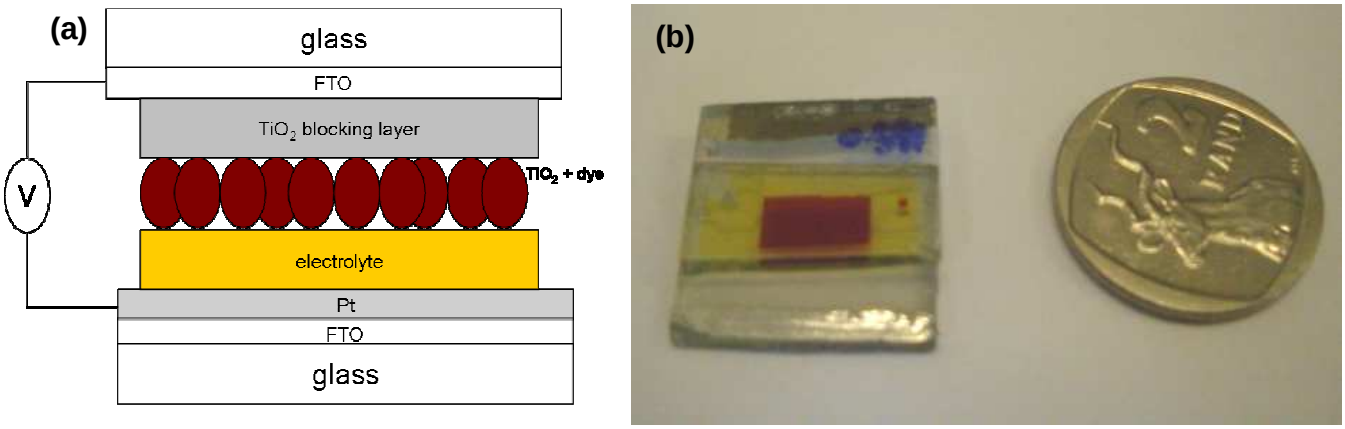

Figure 1: (a) Schematic representation of the structure of a DSC and (b) image of a fully assembled cell

During operation light is absorbed by the dye molecules, resulting in the generation and transfer of an electron from dye molecule to the TiO_2 nanoparticle. The electron then moves through the film of nanoparticles to reach the FTO. Thereafter the electron conducts through a load (e.g. light bulb) towards the Pt/FTO/glass counter-electrode. The negatively charged I^- ion present in the I^-/I_3^- electrolyte then interacts with the positively charged dye molecule, where after the positively charged I_3^- reacts with the electrons at the Pt-coated counter electrode and in so doing, complete the electrical circuit of the cell.

3. Results and discussion

Figure 2 shows SEM images of the TiO_2 nanotubes synthesised at an operating voltage of 60 V and a 200 ml electrolyte solution consisting of 2 wt% H_2O + 0.3 wt% NH_4F + EG. As shown in figure 2 (a), the nanotubes have well defined pores and are detached from each other. At closer inspection it was found that the nanotube diameter increased at a growth rate, f_g of 2.3 nm/V (Cummings et al., 2010). Hence at an operating voltage of 60 V nanotubes with diameters in excess of 100 nm were synthesized. Figure 2 (b) shows a cross-section SEM micrograph, obtained by means of focused-ion beam scanning electron microscopy (FIB-SEM) analyses, and shows that the tubes possess lengths greater than 10 µm, when synthesised at the above stated anodisation bath conditions. Figure 2 (c) shows that the nanotubes have closed bottoms with a hexagonal structure. This hexagonal ordering stems from the hexagonal crystal structure of the anatase TiO_2 crystallites, which constitutes the walls of the nanotubes, as shown by the HR-TEM image of figure 2 (d). The electron microscopy results presented show that the physical dimensions of the nanotubes can be controlled by having accurate control over the experimental conditions during the anodisation synthesis process. This is an important achievement as it is well-known that the physical dimensions of the individual nanotubes play a major role in the performance of the DSC (Macak et al., 2007).

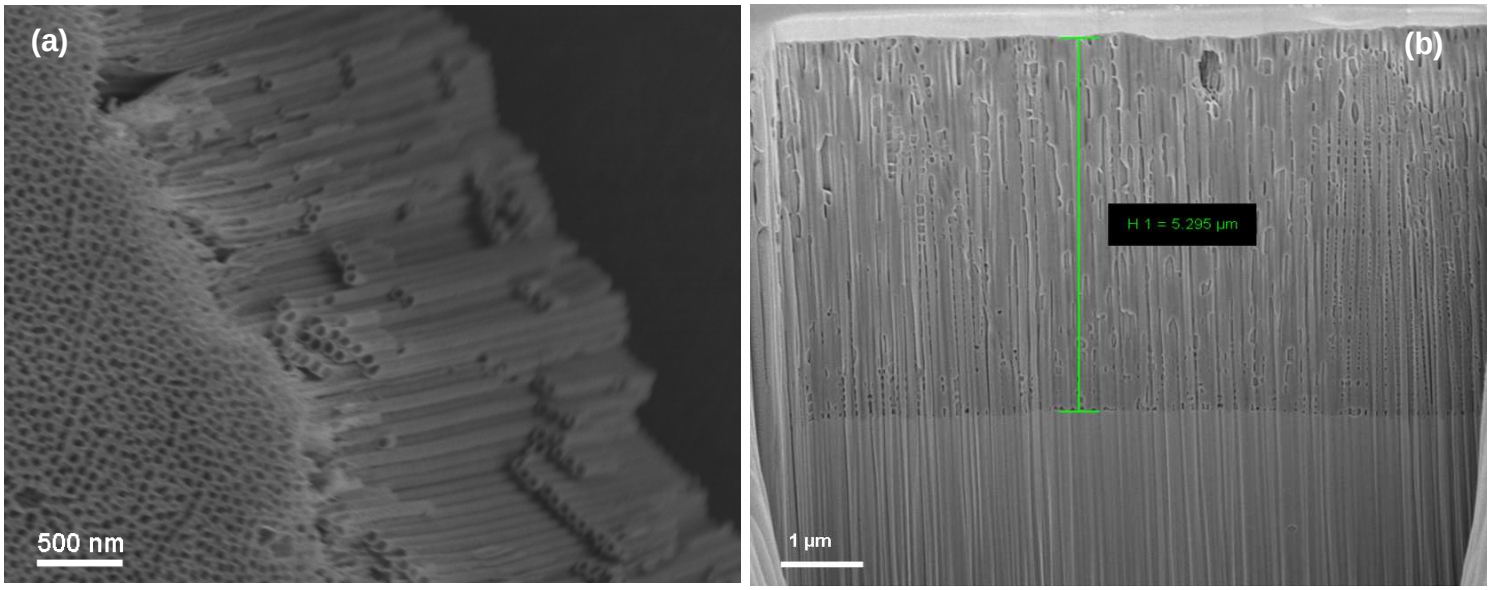

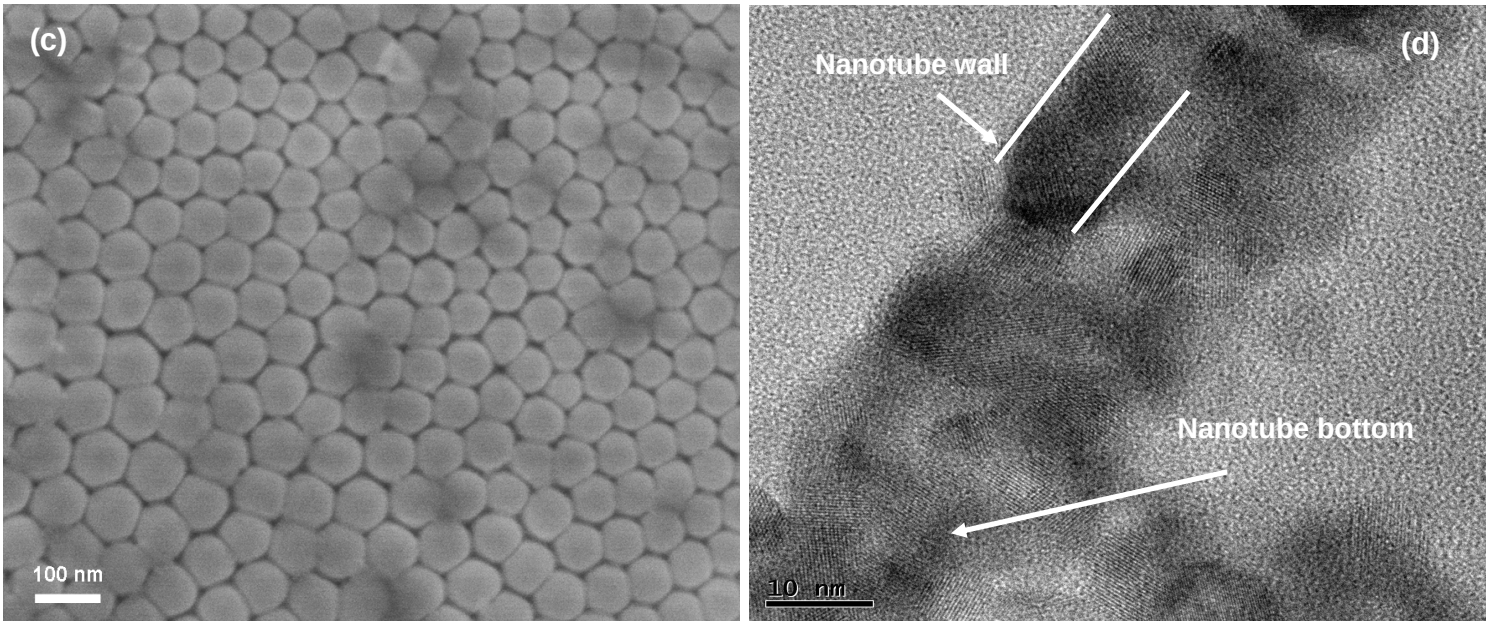

Figure 2: SEM micrographs of (a) aligned TiO_2 nanotubes (b) nanotubes with lengths greater than 10 µm (c) the hexagonally shaped nanotube bottom and (d) TEM micrograph of a TiO_2 nanotube, showing its internal structure

Figure 3 compares AFM height micrographs of a film of TiO_2 nanoparticles to that of a film of nanotubes. A roughness analysis performed on these height images reveals a mean surface area roughness of 155 nm for a 1 x 1 cm^2 film of nanotubes, compared to a mean roughness of 16 nm for a film of TiO_2 nanoparticles. The surface roughness is an important parameter to consider, as a rougher surface area enhances dye adsorption thereby resulting in better light harvesting by the DSC.

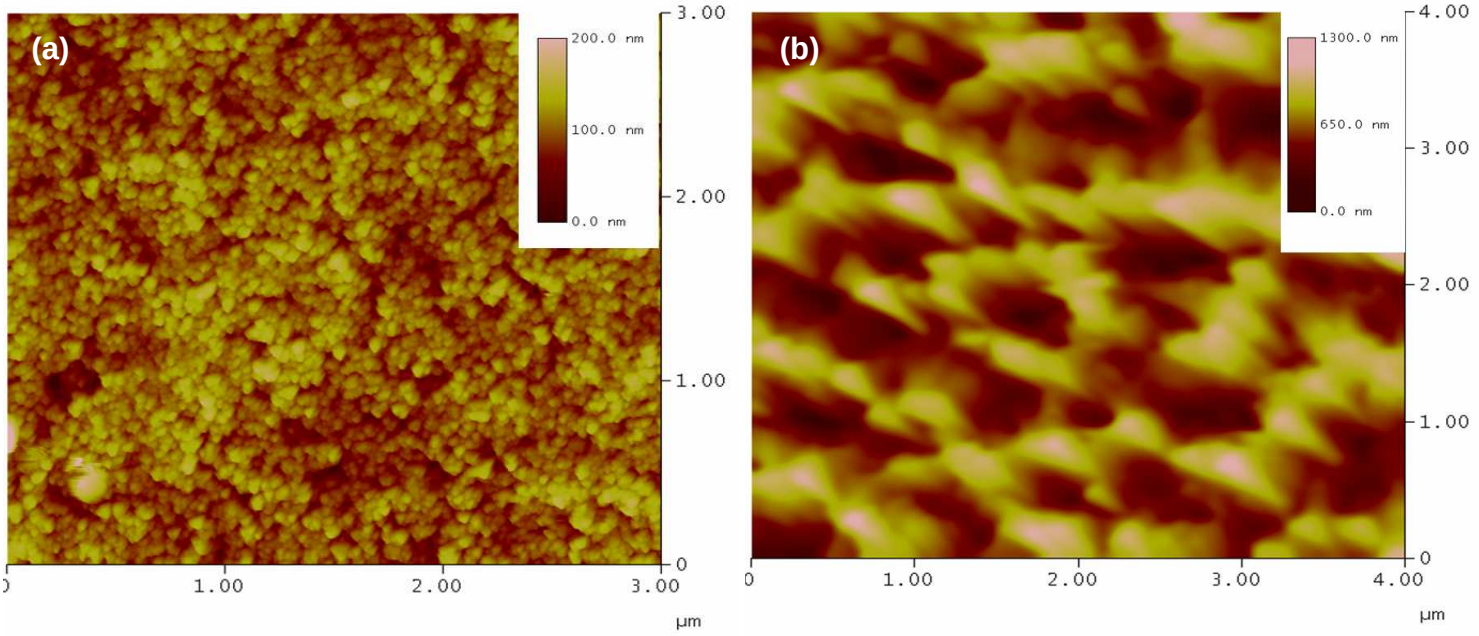

Figure 3: AFM height micrographs of a layer of (a) TiO_2 nanoparticles and (b) TiO_2 nanotubes

Figure 4 (a) plots the XRD diffractograms of the nanotubes. It was found that the nanotubes produced by the anodisation process (i.e. as-synthesised) are amorphous with only diffraction peaks of the Ti substrate visible, as shown in figure 4. Hence, the tubes were annealed at 450ºC for 3 hours in air at atmospheric pressure, which resulted in their crystallisation in the anatase TiO_2 phase. Anatase TiO_2 is the preferred allotrope of TiO_2 as it possesses superior photo-catalytic properties needed for application in DSCs.

The j-V curves, under light illumination, of DSCs based on TiO_2 nanoparticles and nanotubes are shown in figure 4 (b). Three different solar cells are presented in this study, namely two DSCs with a TiO_2 nanoparticle film thickness of respectively 10 (10NP-DSC) and 15 µm (15NP-DSC), and a DSC with a TiO_2 nanotube layer of thickness ~ 15 µm (15NT-DSC). The results plotted are the averaged results from 5 solar cells of each type. The j-V characteristics of a DSC, under forward bias, can be modeled by the real-life one-diode equation, given by

$$j = j_{sat}\exp\left(\frac{e_0 V - e_0 R_s j}{m_D k T}\right) - j_{sat} + j_{sc} + \frac{V - R_s j}{R_{sh}} \qquad (1)$$

where j_{sat} = saturation current
j_{sc} = short circuit current
R_s = series resistance
R_{sh} = shunt resistance, and
m_D = ideality factor.

From figure 4 (b) the most significant differences between cells made respectively with nanotubes and nanoparticles are observed under short-circuit conditions, i.e. where V = 0 (j = j_{sc}) from equation (1). It can be seen that the j_{sc} values for DSCs fabricated with nanotubes as the charge transport medium, are significantly lower than that of cells made with a film of TiO_2 nanoparticles. The j_{sc} value of a solar cell gives direct indication of the light absorption ability of the cell, with low j_{sc} values implying poor light absorption. Hence, in this case, it can be seen that DSCs with a layer of nanotubes incorporated in its structure absorbs less sunlight than a DSC employing a film of TiO_2 nanoparticles. This is attributed to the low surface area of a film of nanotubes compared to that of a film of nanoparticles with the same film area and thickness. The low surface area, in turn, results in decreased dye-adsorption by the nanotubes, which ultimately yields poor light absorption seeing that the dye is responsible for light absorption. In other words, solar cells employing TiO_2 nanotubes capture less sunlight, hence produce smaller currents.

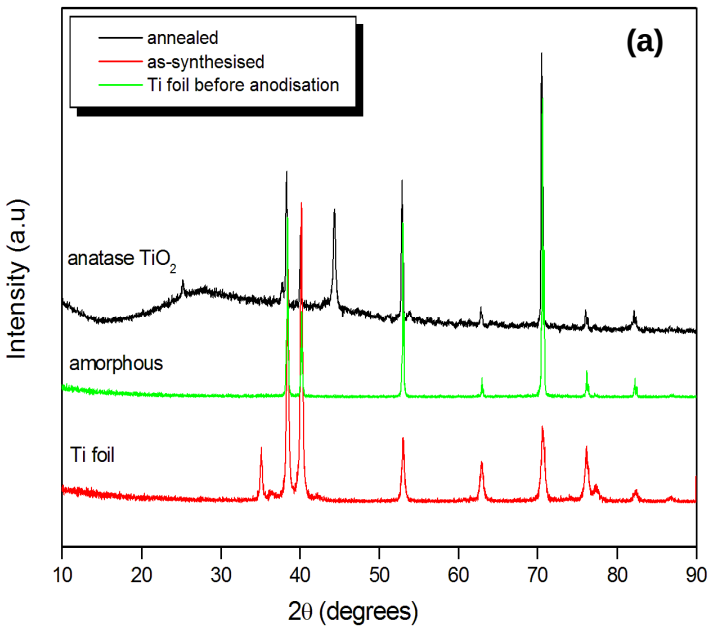

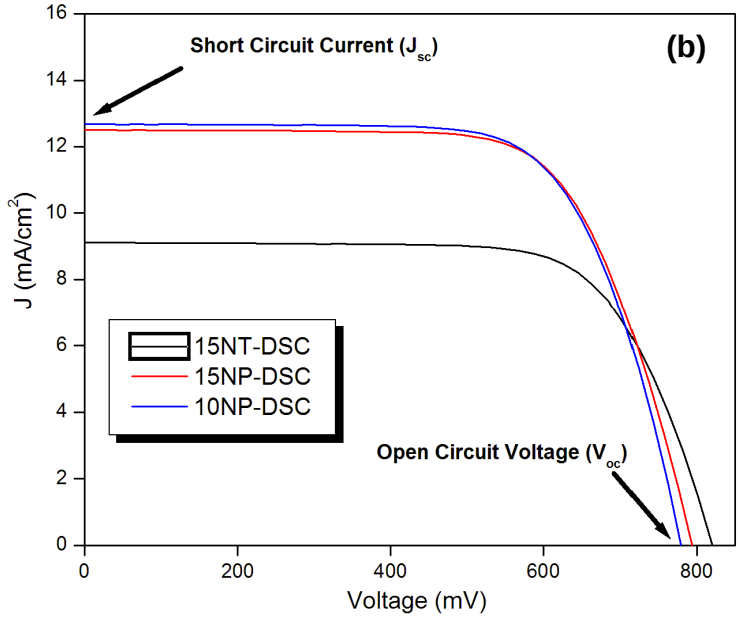

Figure 4: (a) XRD patterns of the TiO_2 nanotubes annealed at 450 ºC for 3 hours in air at atmospheric pressure. For comparison, the XRD patterns of the Ti substrate and the as-synthesised, amorphous TiO_2 nanotubes are also included for reference. (b) j-V curves of the DSCs manufactured with nanoparticles and nanotubes

However, what the nanotube-based DSC lacks in light absorption, it makes up for in charge transport. Under open-circuit conditions, i.e. where j = 0 (V = V_{oc}) it can be seen that nanotube-based DSCs possess greater V_{oc} values, which implies a reduction in charge recombination and ultimately greater charge transport to the charge collecting contacts. To give a holistic description of the performance of the two types of cells, one has to consider, not only the light-harvesting and charge transport properties of the cell, but rather the overall light-to-charge conversion efficiency, η, of the solar cell. In general, η is given by

$$\eta = \left(\frac{j_{sc} V_{oc}}{P_{in}}\right) \times FF \qquad (2)$$

where P_{in} is the incident irradiance in W/cm^2 (taken as 100 mW/cm^2) and FF the fill factor, given by $\frac{P_{max}}{j_{sc} V_{oc}}$, with P_{max} the maximum power output of the cell in W/cm^2. Using equation 2 and the data obtained from figure 4 (b), conversion effiencies of 5.34, 6.88 and 6.94% were obtained for cells 15NT-DSC, 10NP-DSC and 15NP-DSC respectively. Thus it can be seen that the solar cells containing a layer of nanotubes have a markedly lower efficiency than their nanoparticle counterpart. As discussed above, this is mainly attributed to the low surface area of the nanotube, which can be traced back to the TiO_2 nanotube synthesis process employed. More specifically, further work is required in perfecting the TiO_2 nanotube synthesis process in order to produce a layer of nanotubes with greater physical dimensions, i.e. nanotube diameter and wall thickness. Notwithstanding, it was shown that DSCs with layers of nanotubes instead of nanoparticles, have greater charge transport properties, which has traditionally been the Achilles heel of the DSC.

4. Conclusions

In this work the photovoltaic performance of DSCs with a layer of TiO_2 nanotubes as the charge transport medium was compared to that of a conventional DSC. It was found that nanotube-based DSCs suffer from low light absorption, which was attributed to the low surface area of the film of nanotubes. The low light

absorption further implied that the cell had a low light-to-electricity conversion efficiency. In contrast, it was shown that these novel solar cells offer greater charge transport compared to conventional DSCs.

5. References

CUMMINGS, F.R., LE ROUX, L.J., MATHE, M.K., & KNOESEN, D. 2010. Structure-induced optical properties of anodised TiO_2 nanotubes. *Materials, Chemistry and Physics*, (In Press) doi:10.1016/j.matchemphys.2010.06.024.

MACAK, J.M. TSUCHIYA, H., GHICOV, A., YASUDA, K., HAHN, R., BAUER, S., & SCHMUKI, P. 2007. TiO_2 nanotubes: Self-organised electrochemical formation, properties and applications. *Current Opinion in Solid State and Materials Science*, 11:3-18.

MOHAPATRA, S.K., MISRA, M., MAHAJAN, V.K., RAJA, K.S. 2007. A novel method for the synthesis of titania nanotubes using sonoelectrochemical method and its application for photoelectrochemical splitting of water. *Journal of Catalysis*, 246:362-369.

MOR, G.K., VARGHESE, O.K., PAULOSE, M., SHANKAR, K., & GRIMES, C.A. 2006. A review on highly ordered, vertically oriented TiO_2 nanotube arrays: Fabrication, material properties, and solar energy applications. *Solar Energy Materials & Solar Cells*, 90:2011-2075.

O'REGAN, B., & GRATZEL, M. 1991. A low-cost, high-efficiency solar cell based on dye-sensitised colloidal TiO_2 films. *Nature*, 353:737-740.

PARK, H., KIM, W.-R., JEONG, H.-T., LEE, J.-J., KIM, H.-G., CHOI, W.-Y. 2010. Fabrication of dye-sensitized solar cells by transplanting highly ordered TiO_2 nanotube arrays. *Solar Energy Materials & Solar Cells*, (In Press) doi:10.1016/j.solmat.2010.02.017.

PAULOSE, M., SHANKAR, K., VARGHESE O.K., MOR. G.K., & GRIMES, C.A. 2006. Application of highly-ordered TiO_2 nanotube-arrays in heterojunction dye-sensitised solar cells. *Journal of Physics D: Applied Physics*, 39:2498-2503.

TOYODA, T., SANO, T., NAKAJIMA, J., et al. 2004. Outdoor performance of large scale DSC modules. *Journal of Photochemistry and Photobiology A: Chemistry*, 164:203-207.